The mechanism of *N*-vinylindole formation *via* tandem imine formation and cycloisomerisation of *o*-ethynylanilines†

Danielle F. Kennedy,[a] Ainara Nova,[b] Anthony C. Willis,[c] Odile Eisenstein*[b] and Barbara A. Messerle*[a]

Received 29th July 2009, Accepted 17th September 2009
First published as an Advance Article on the web 14th October 2009
DOI: 10.1039/b915269e

The reaction of 2-(2-phenylethynyl)aniline with acetone in presence of $[IrCp^*Cl_2]_2$ has previously been found to yield a vinyl indole derivative and not the indole expected to form following a hydroamination reaction. Experimental data, including labelling studies, isolation and solid state structure determination of a reaction intermediate together with DFT calculations were used to develop a mechanism for the formation of the vinyl indole. In the mechanism proposed, acetone plays a significant role in several steps of the reaction path, participating in the fragmentation of the dinuclear Ir complex and the formation of the reactive form of the catalyst as well as blocking the formation of the expected hydroamination product by coordination to the Ir catalyst. Coordinated acetone reacts with the aniline to form an imine derivative, which yields the final product following proton transfer promoted by acetone. The proposed mechanism is in good agreement with the experimental data.

Introduction

Substituted indoles have become important pharmaceutical agents because of the well documented biological activity exhibited by compounds containing an indole motif.[1,2] Indoles are said to have a "privileged" structure due to their ability to bind with high affinity to many biological receptors.[3] Numerous methods have been developed for the synthesis of substituted indoles, however, the efficient synthesis of suitably modified indoles remains a challenge to the synthetic chemist.[3,4] In particular, it remains difficult to synthesise many simple unsubstituted indoles. Bulky, electron withdrawing or donating substituents on indole have been widely used because they have significant directing effects on the efficiency of synthesis, blocking, activating or deactivating various positions to substitution.[5]

Increasingly, metal complexes containing Ir(III) metal centres are being investigated as catalysts for a variety of transformations. Work by Bergmann *et al.* with the complexes $Cp^*(PMe_3)Ir(CH_3)(OTf)$, and $Tp^{Me2}(PMe_3)Ir(CH_3)(OTf)$ illustrated the ability of Ir(III) complexes to effect C–H activation.[6,7] Crabtree *et al.* have utilised an Ir(III) hydride complex to achieve alkyne insertion into a Ir-H, and also catalyse the intramolecular hydroamination and hydroalkoxylation of alkynes.[8,9] $[Cp^*IrCl_2]_2$ is also effective as a catalyst for a variety of transformations, such as the hydroborylation of styryl sulfonamides,[10] the *N*-alkylation of amines with alcohols[11,12] and the transfer hydrogenation of ketones[13] and quinolines.[14]

N-vinyl indoles have been used as monomers in the production of poly(*N*-vinyl indoles) which found application in the production of photorefractive materials.[15] There are, however, relatively few reports of the synthesis of *N*-vinyl indoles.[16-18] Work by Li *et al.* utilises a gold catalysed synthesis of *N*-vinyl indoles *via* a Au(III) catalysed double hydroamination of *o*-alkynylanilines and terminal alkynes.[16] Investigation into the mechanism of this reaction indicated that the first step of this reaction was intermolecular hydroamination between the aniline and terminal acetylene to generate the imine, followed by intramolecular hydroamination.[16] Recently we reported the Ir(III) catalysed synthesis of *N*-(2-methylvinyl)-2-phenylindole **2** *via* the cyclisation of 2-(2-phenylethynyl)aniline **1** by the Ir(III) dimer, $[IrCp^*Cl_2]_2$, Scheme 1a.[19] This reaction was an unexpected outcome, and it was presumed to be the direct result of either a hydroamination reaction or a modified hydroamination reaction incorporating one molecule of the solvent acetone. These results

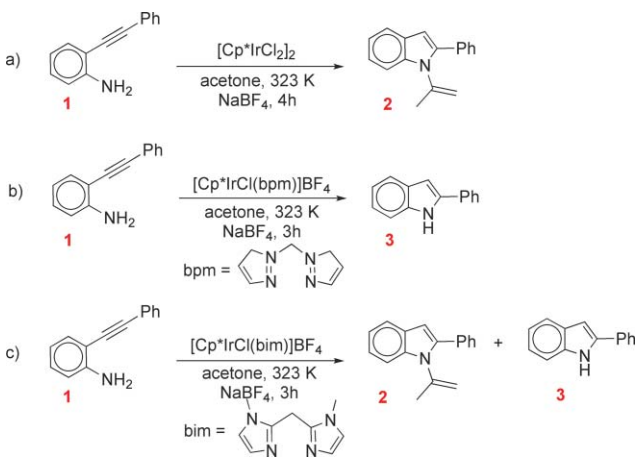

Scheme 1

[a]*School of Chemistry, The University of New South Wales, Sydney N.S.W. 2052, Australia. E-mail: b.messerle@unsw.edu.au; Fax: ++61-2-9385-6141*
[b]*Institut Charles Gerhardt, Université Montpellier 2, CNRS 5253, cc 1501, Place Eugène Bataillon, 34095, Montpellier Cedex 5, France. E-mail: Odile.Eisenstein@univ-montp2.fr*
[c]*Research School of Chemistry, The Australian National University, Canberra A.C.T. 0200, Australia*

† Electronic supplementary information (ESI) available: Computational results obtained with cationic Ir species. Optimized structures of all stationary points with their absolute energies calculated in solvent. CCDC reference number 741292. For ESI and crystallographic data in CIF or other electronic format see DOI: 10.1039/b915269e

contrast with the more commonly observed hydroamination cyclisation reaction without addition of acetone, forming the indole product **3** (Scheme 1b), and the alternate Ir(III) catalysed cyclisation reported recently where a mixture of **2** and **3** was formed (Scheme 1c).[19] This reaction provides a simple method for the synthesis of the previously unknown vinyl indole **2**, and was discovered as a part of our investigations into new catalysts for hydroamination. Here we describe our studies into the mechanism of this reaction.

Results and discussion

The catalyst promoting the formation of vinyl indole (**2**) by reaction of 2-(2-phenylethynyl)aniline (**1**) with acetone was the Ir(III) dimer, $[IrCp^*Cl_2]_2$ (Scheme 1a). When 2-(2-phenylethynyl)aniline **1** was reacted with 2.8 mol% $[IrCp^*Cl_2]_2$, 95% in acetone, conversion to vinyl indole **2** was observed in 20 h at 323 K. When $NaBF_4$ was included with the catalyst a significantly enhanced rate of reaction (from 20 to 4 h) was observed. Two possible routes for the formation of compound **2** are shown in Fig. 1 (Pathways I and II). The first route (Pathway I) involves initial hydroamination leading to the indole intermediate **A** followed by the reaction of **A** with acetone. In this pathway the metal does not play an active role in the addition of acetone. The second route (Pathway II) involves initial reaction of the acetone with the aniline **1** to generate an imine intermediate **B**, which then undergoes metal catalysed cyclisation to generate the vinyl indole product **2**. In this work, we have combined experimental and computational studies to investigate if one of these pathways is operative or if other elementary steps should be included.

Deuterium labelling study

To gain further understanding of the catalysed formation of *N*-(2-methylvinyl)-2-phenylindole **2**, Scheme 1a, the reaction of $[IrCp^*Cl_2]_2$ with **1** was performed using acetone-d_6 and monitored *via* ^{1}H NMR spectroscopy. When 2-(2-phenylethynyl)aniline **1** was treated with 2.8 mol% $[IrCp^*Cl_2]_2$ in acetone-d_6 at 323 K (Fig. 2), conversion of **1** to **2** was achieved in *ca.* 20 hours with 100% deuteration of the methylvinyl group. This shows that the methyl vinyl group does originate from the acetone. Complete deuteration at C3 on the indole ring was also observed. This is consistent with Pathway II, where the proton at C3 of the indole ring derives directly from the deuterated acetone reactant. The hydroamination pathway (Pathway I, Fig. 1) would result in protonation at C3 of the indole, with the proton derived from N–H of the aniline.

The ^{1}H NMR spectra were examined to detect the presence of any of the possible intermediates **A** or **B**, or free 2-phenylindole (**3**) (Fig. 2). No resonances due to the stable 2-phenylindole (**3**) or the metal bound indole intermediate **A** were observed at any time during the course of the reaction further suggesting that Pathway I is not operative. Pathway II was not excluded from consideration, even though the imine intermediate **B** was not observed experimentally, as rapid cyclisation would consume **B** immediately.

The reaction of **1** with $[IrCp^*Cl_2]_2$ and $NaBF_4$ was also performed using acetone-d_6 on a small scale and monitored *via* ^{1}H NMR spectroscopy. The aniline, **1**, was reacted with 2.4 mol% $[IrCp^*Cl_2]_2$ and $NaBF_4$ in acetone-d_6 at 323 K. The reaction proceeded to more than 95% conversion in under 4 h, a significantly faster rate than in the absence of $NaBF_4$. The ^{1}H NMR spectra from this reaction were examined and also

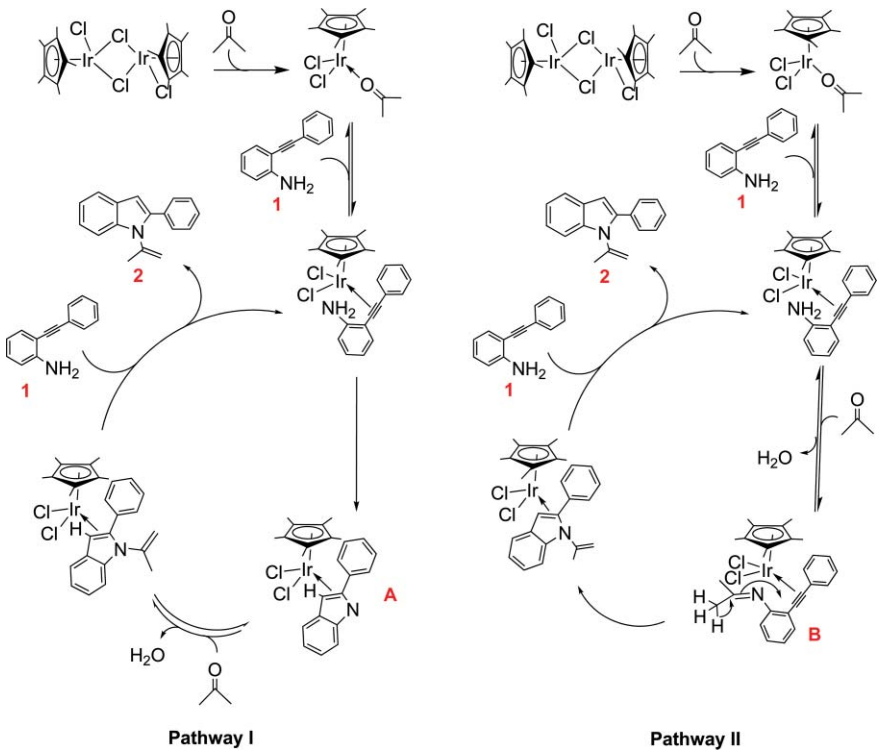

Fig. 1 Possible reaction routes for the generation of **2** from **1** in acetone indicating Pathway I *via* indole intermediate **A** and Pathway II *via* imine intermediate **B**.

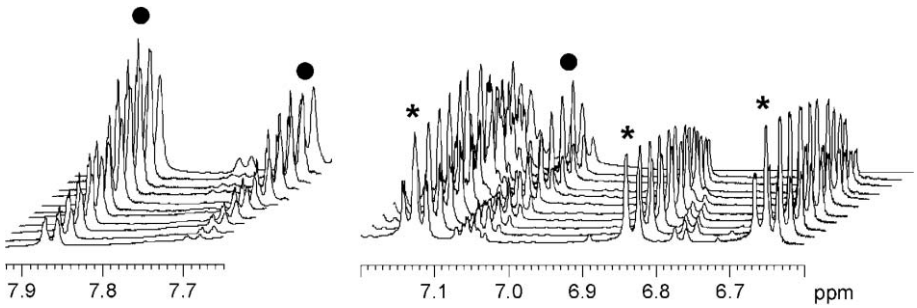

Fig. 2 Stacked plots of the ^{1}H NMR spectra for the catalysed reaction of **1** to **2** by 5.7 mol% $[IrCp^*Cl_2]_2$ over time. The stars indicate resonances due to **1** and the circles indicate resonances due to **2**.

failed to show the presence of 2-phenylindole **3** or any imine intermediate at any stage of the reaction. The combination of $[IrCp^*Cl_2]_2$ and $NaBF_4$ as catalyst gave an identical deuteration pattern to that observed when $[IrCp^*Cl_2]_2$ alone was used as catalyst. This suggests that the addition of $NaBF_4$ accelerates the reaction without modifying its mechanism.

Reactions of 2-phenylindole (3)

In order to rule out Pathway I completely, 2-phenylindole **3** was heated at 323 K with 5 mol% $[IrCp^*Cl_2]_2$ and $NaBF_4$ in acetone for 18 hours. At the end of the reaction, only the starting material was detected and no discernible decomposition was observed. It is therefore unlikely that the reaction route involves initial hydroamination followed by addition of acetone (Pathway I).

The role of solvent

In order to investigate the role of the solvent on the mechanism depicted in Fig. 1, the reaction of $[IrCp^*Cl_2]_2$ with aniline **1** was tried using the following solvent mixtures: thf-d_8, thf-d_8 in the presence of 1 molar equivalent of H-acetone, and thf-d_8 in the presence of 3.5 molar equivalents of H-acetone.

In the first case, the aniline **1** was reacted in thf-d_8 with 2.5 mol% $[IrCp^*Cl_2]_2$ and $NaBF_4$ at 323 K and monitored *via* ^{1}H NMR spectroscopy. After 18 hours neither conversion to 2-phenylindole (**3**) nor decomposition of **1** was observed. The same result was obtained when **1** was heated at 323 K in thf-d_8 with one molar equivalent of H-acetone in presence of $[IrCp^*Cl_2]_2$. However, when the reaction was repeated with the amount of acetone increased to 3.5 molar equivalents, a very slow conversion of the aniline **1** to a mixture of the vinyl indole product **2** and 2-phenylindole **3** (1:2) was observed after 7 hours with a yield of 48%. Therefore hydroamination of **1** yielding **3** (first step of Pathway I) is possible, suggesting that intermediate **A** is accessible in these conditions. However, this reaction appears to be blocked when the solvent is pure acetone. Product **3** is not formed in the absence of acetone, which seems to indicate that acetone is required to break the Ir dimer, $[IrCp^*Cl_2]_2$.

Isolation of $[IrCp^*Cl_2(aniline\text{-}\kappa N)]$ (4)

When the reaction of **1** with acetone was performed with a large amount of $[IrCp^*Cl_2]_2$ (5 mol%) and $NaBF_4$ at 323 K, isolation and characterization of the intermediate $[IrCp^*Cl_2(aniline\text{-}\kappa N)]$ (**4**) was possible. The product, vinylindole **2**, was also isolated from the reaction in a low yield. One of the reasons for the low yield was the significant loss of the vinyl unit from **2** during chromatography, generating 2-phenylindole (**3**). This was confirmed by monitoring the decomposition of **2** in slightly acidic solutions. Acidic decomposition generated **3** quantitatively over a period of several days at room temperature.

The second product, the yellow solid isolated from the reaction, was recrystallised from hexane and CH_2Cl_2 to yield orange crystals of complex **4** of crystallographic quality. The ^{1}H NMR spectrum of complex **4** in acetone-d_6 showed the presence of one molar equivalent of bound Cp* per mole of **1**, and confirmed that the aniline **1** retained both of its hydrogens, with the NH_2 resonance integrating to two protons. The resonance due to the NH_2 of the Ir bound aniline **1** is shifted downfield to 5.80 ppm compared to the NH_2 resonance of the free aniline **1** which occurs at 5.11 ppm. ^{1}H-^{1}H NOESY NMR spectroscopy also showed a clear correlation between the methyl groups of the Cp* unit and the protons of the NH_2 group of the aniline **1** confirming that a complex had been isolated which contained **1** bound to the Ir(III) metal centre.

The solid state structure of **4** was obtained using X-ray crystallography and is shown with thermal ellipsoids at the 30% probability level, Fig. 3. Selected bond lengths and angles for **4** are presented in Table 1 and crystal structure and refinement data are given in the experimental section. The crystallographic asymmetric unit consists of one $[IrCp^*Cl_2(aniline\text{-}\kappa N)]$ molecule and one dichloromethane molecule of solvation. The crystal contains only one enantiomer of the molecule. In solution the compound is

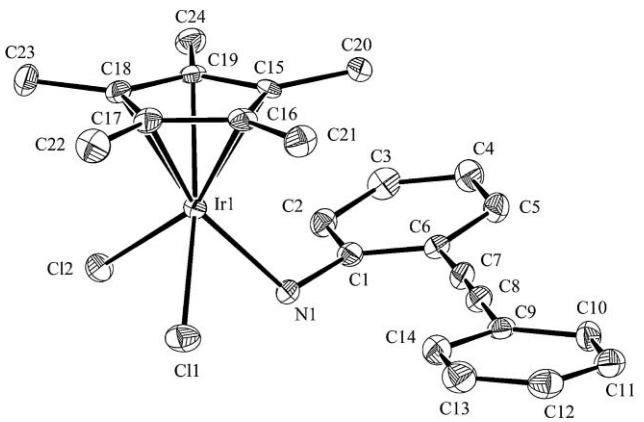

Fig. 3 Anisotropic displacement ellipsoid plot of $[(C_{10}H_{15})IrCl_2(C_{14}H_{11}N)]$, **4**, with labeling of selected atoms. Ellipsoids show 30% probability levels. Hydrogen atoms have been deleted for clarity.

Table 1 Selected bond lengths (Å) and bond angles (°)[a] for the inner coordination sphere of **4**

Atomic distance (Å)			
Ir1–Cl1	2.4157 (8)	Ir1–C15	2.172 (3)
Ir1–Cl2	2.4179 (8)	Ir1–C16	2.153 (3)
Ir1–N1	2.179 (2)	Ir1–C17	2.155 (3)
C7–C8	1.192 (4)	Ir1–C18	2.158 (3)
C1–N1	1.433 (4)	Ir1–C19	2.141 (3)
Bond angle (°)			
Cl1–Ir1–Cl2	91.00 (3)	C6–C7–C8	176.5 (4)
Cl1–Ir1–N1	79.31 (7)	C7–C8–C9	178.5 (4)
Cl2–Ir1–N1	81.60 (7)	Ir1–N1–C1	119.44 (19)

[a] Estimated standard deviation in the least significant figure are given in parentheses.

presumably racemic but it appears to have spontaneously resolved on crystallisation. The solid state structure of **4** is analogous to the structure previously reported for [IrCp*Cl_2(NH_2Ph)],[20] and all bond distances are comparable. The only significant difference between the two complexes is a slightly smaller Ir1–N1–C1 angle 119.44(19)° in **4** compared 121.40° for [IrCp*Cl_2(NH_2Ph)].

The fact that substrate **1** is N-bound to the Ir(III) metal centre, rather than π-bound is consistent with the amine being a stronger Lewis base than the alkyne. Structural rearrangement would be necessary for the reaction to proceed to completion.

Reactivity of [IrCp*Cl_2(aniline-κ*N*)] (4)

In order to probe if **4** is an intermediate for the formation of **3**, complex **4** was dissolved in CD_2Cl_2, heated at 323 K and monitored *via* ^{1}H NMR spectroscopy. No conversion to 2-phenylindole **3** was observed, indeed no change was observed at all in the complex over a period of 18 h at 323 K. Coordinated aniline, as in **4**, cannot achieve hydroamination because the alkyne is not activated towards nucleophilic addition, and also because the nucleophilicity of the amine has been removed. This is in agreement with the proposal by Crabtree *et al.* that coordination through the nitrogen of ethynylanilines leads to unproductive binding rather than hydroamination.[9] However the formation of **3** when the reaction takes place with 3.5 molar equivalents of acetone in thf suggests that the change in the coordination from κ^1(N) to η^2(CC) has to be possible at least in the presence of acetone. Therefore, the acetone appears to be also necessary for the hydroamination process, not only for the fragmentation of the Ir dimer.

Complex **4** was also heated in acetone-d_6 at 323 K and within 3 minutes complete conversion of the metal complex was observed. An organic product was identified in the reaction mixture as *N*-(2-methylvinyl)-2-phenylindole (**2**) by ^{1}H NMR while precipitation of [IrCp*Cl_2]$_2$ occurred as red crystals. This shows that **4** is an active species in acetone and is on the reaction path to yield **2**.

Computational studies

Thermodynamic considerations. The main difference between Pathways I and II as they are described earlier in the paper (Fig. 1) is that, in the former, the reaction starts with the cyclisation of aniline **1** to give indole **3**, while in the latter the reaction starts with the formation of the imine (**5**). The thermodynamic values determined for the transformations of the organic molecules alone are shown in Scheme 2 for both pathways. The formation of the final vinylindole (**2**) *via* the 2-phenylindole (**3**) is unlikely because of the endothermicity of the **3** to **2** transformation (17.7 kcal mol^{-1}). Therefore the formation of this species should avoid formation of **3** which would act as a trap. This agrees with the experimental data that showed that in neat acetone and in the presence of catalyst, **3** is not converted to **2** and allows us to disregard Pathway I as a possible route for the formation of **2**.

Pathway II (Fig. 1) starts with the formation of intermediate **B** where the imine coordinated to Ir comes from the reaction of **1** with acetone. The organic reaction of **1** + acetone → **5** + H_2O is moderately endothermic as shown in Scheme 2, but the strong thermodynamic drive associated with the cyclisation to give **2** makes the step from **1** to **5** energetically feasible. As the condensation of an amine and acetone can take place in the absence of any metal, we did not study the condensation reactions, and we compare the energy profile for the imine cyclisation with that obtained for the amine cyclisation.

As has been suggested by the experiments the fragmentation of the Ir dimer, [IrCp*Cl_2]$_2$, is assisted by acetone. This process has not been studied computationally and the unsaturated CpIrCl_2 has been considered as the reactive form of the catalyst. This fragment can coordinate acetone, aniline (**1**) or imine (**5**).

Cyclisation of the amine *vs.* the imine. The following notation has been introduced. All species derived from the amine cyclisation (*i.e.* Pathway I, Fig. 1) will be labelled with letter **a**, while all species originating from the imine (*i.e.* Pathway II, Fig. 1) will be labelled with the letter **i**.

The amine and imine cyclisations start with the coordination of **1** and **5** to [CpIrCl_2], respectively. The unsaturated CpIrCl_2 fragment coordinates preferentially the most Lewis basic site of either **1** or **5**. It thus coordinates preferentially to the nitrogen to form a κ^1(N) complex rather than to the alkyne to form a η^2(CC) complex. Hence, complex **a1** (see Scheme 3) is the initial reactant for the amine cyclisation and it is also used as the reference point for all energies throughout the remainder of the paper. Species **i1**

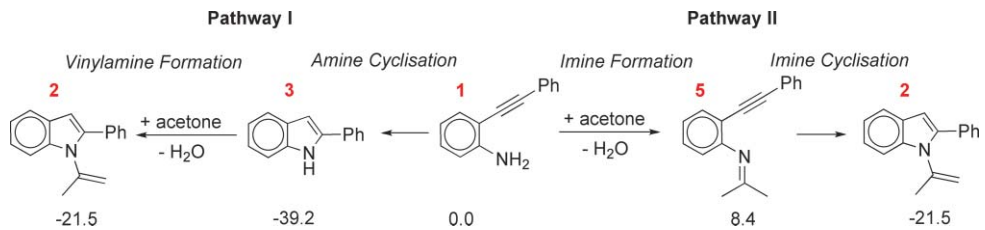

Scheme 2 Reactions that could account for the formation of vinylindole **2** *via* Pathway I (left side) and Pathway II (right side) in Fig. 1. Energies are given in kcal mol^{-1} and include the solvent (acetone) effect.

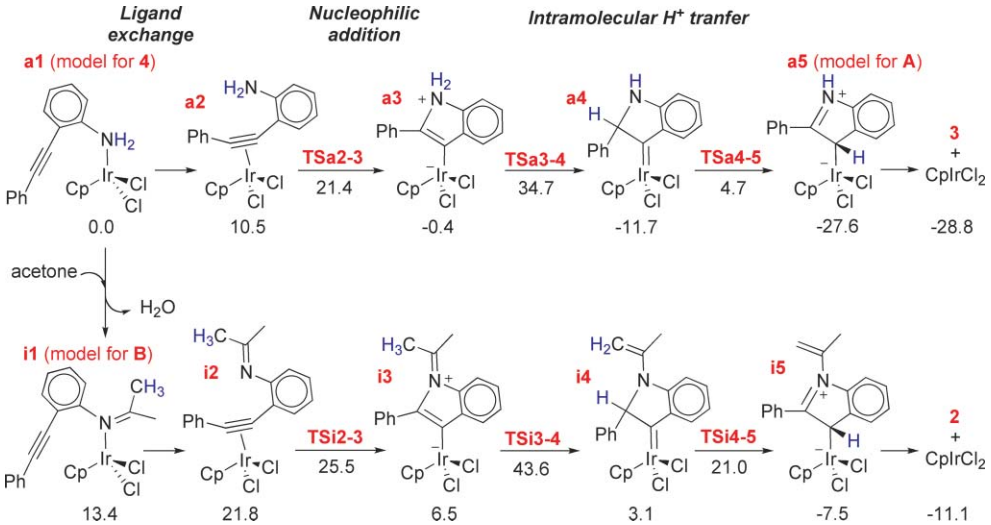

Scheme 3 Cyclisation mechanism of amine (top) and imine (bottom) including the intramolecular proton transfer. Energies are given relative to **a1**, in kcal mol^{-1} and include the solvent (acetone) effect.

is the reactant for the imine cyclisation. It is 13.4 kcal mol^{-1} higher in energy than **a1** because the formation of the imine and water from the amine and acetone is endothermic and because the imine nitrogen is a weaker Lewis base than the amine nitrogen.

From **a1** and **i1**, the first cyclisation mechanism that we considered is shown in Scheme 3. The mechanism can be divided in three steps: 1) change from N coordination to alkyne coordination; we did not search for a transition state in this step, which is a simple ligand substitution; 2) intramolecular nucleophilic addition of N to the activated alkyne to form the 5-membered ring; and 3) intramolecular proton transfer to replace the Ir-C bond by a C-H bond of the final products **3** or **2**. In the amine cyclisation route the proton originates from the NH_2 group, and in the imine cyclisation route the proton originates from the CH_3 group of acetone. In the first instance, we selected this intramolecular proton transfer because it readily provides a suitable explanation for the selective deuteration at C3 of the indole when using acetone-d_6.

The nucleophilic addition of the nitrogen to the alkyne (Scheme 3) starts with a change in the coordination of the amine or imine, from κ^1(N) to η^2(CC). This process is energetically easier from **i1** to **i2** (8.4 kcal mol^{-1}), than from **a1** to **a2** (10.5 kcal mol^{-1}) because the imine is less basic than the amine. The next step, which produces the 5-membered ring, is the nucleophilic addition of a Lewis base to an activated multiple bond. Remarkably, the energy barrier for the cyclisation step is lower with imine, **TSi2-3** (3.7 kcal mol^{-1}) than with amine, **TSa2-3** (10.9 kcal mol^{-1}). This is due to the fact that the N lone pair of **a2** is conjugated with the phenyl group and a 90° rotation of the NH_2 group around the C-N bond is needed for the amine to add to the alkyne. Such rotation is not needed with **i2**. Despite the fact that the energy barrier for the cyclisation step is lower in the case of the imine cyclisation route, the energies of the transition states for amine and imine cyclisation are close in energy relative to reactants (energy of 21.4 kcal mol^{-1} for **TSa2-3** and of 25.5 kcal mol^{-1} for **TSi2-3**), and the energy of the transition state for the amine cyclisation is slightly lower. Thus, while the cyclisation of the imine **5** is energetically easier than that of the amine **1**, the energy required to form **5** disfavours the cyclisation step in Pathway II.

To form the final product, either **2** or **3**, a proton has to be transferred to C3 of the indole. As indicated earlier, the source of the proton is geometrically far from C3 since the proton should come either from the nitrogen in the case of Pathway I, Fig. 1, (*via* the amine) or from one of the methyl groups of the iminium group. No direct proton intramolecular transfer from reactant to product was identified and, in all cases, the only possible routes found using the calculations were multi-step processes. In the case of Pathway I, a two-step process is necessary to form **3**: the proton migrates from N to C2 of the indole (from **a3** to **a4**) with an energy barrier of 35.1 kcal mol^{-1} followed by a transfer from **a4** to **a5** with a rather low energy barrier of 16.4 kcal mol^{-1}. In the case of the imine, a similar path takes place between **i3** and **i5**, but the TS energy for the first step has an even higher energy (**TSi3-4** = 43.6 kcal mol^{-1}).[21]

These intramolecular proton transfers with high energy barriers are unlikely to occur. In another hydroamination study reported recently, it is proposed that the proton transfer is assisted by the counterion (OTf$^-$),[22] and in this case the BF_4^- anion is not very likely to play this role. The species **a3** or **i3** are rather acidic, and intermolecular proton transfer to a molecule which can act as a base such as the amine or the acetone, is more likely to occur. Although the amine is more basic than acetone, the molar ratio of acetone: **1** is large, making the acetone a candidate for promoting the transfer. In addition the stereoselectivity of the proton transfer from acetone to C3, demonstrated by the use of acetone-d^6, can only be understood if acetone assists the proton transfer. Therefore we considered this possibility and the energies obtained are shown in Scheme 4.

The proton transfer from either **a3** or **i3** to acetone gives an anionic Ir complex and a cationic protonated acetone which can form ion pairs. Either for **a3** or for **i3**, we found that the transition state for forming the ion pair **a4ass** or **i4ass** (**ass** for assisted by the solvent) is very close in energy to that of the ion pairs themselves. Likewise the energy of the transition state for transferring the proton from the protonated acetone to C3 is almost at the same energy as the ion pair. The calculations show that **a4ass** is only 6.0 kcal mol^{-1} above **a3** and that **i4ass** is only 17.6 kcal mol^{-1}

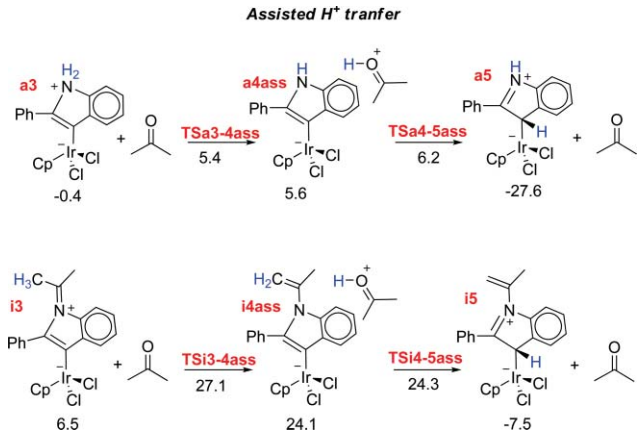

Scheme 4 Proton transfer of amine (top) and imine (bottom) assisted by acetone. Energies are given relative to **a1**, in kcal mol^{-1} and include the solvent (acetone) effect.

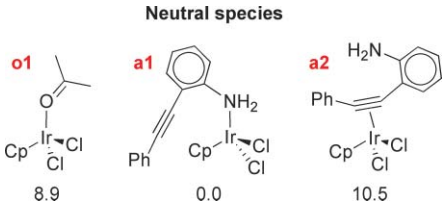

Scheme 5 Possible reactants for the cyclisation of amine or formation of imine. Energies are given relative to **a1**, in kcal mol^{-1} and include the solvent (acetone) effect.

above **i3**. These two ion pairs thus are significantly lower in energy than the transition states **TSa3-4** or **TSi3-4**. Consequently, an intermolecular proton transfer assisted by acetone is preferred over an intramolecular proton transfer. This role of the acetone can explain why the experimental complex **4** (modelled by **a1**) does not give hydroamination in pure CD_2Cl_2 solvent and requires at least 3.5 molar equivalents of acetone.

Looking at the whole path, it appears that the highest transition state on Pathway I for the formation of the amine **3** (**TSa2-3** = 21.4 kcal mol^{-1}) is slightly lower than the highest transition state for the formation of the vinyl imine **2** on Pathway II (**TSi3-4ass** = 27.1 kcal mol^{-1}). Thus at least a mixture of **2** and **3** should be observed in the reaction of **1** with $[IrCp^*Cl_2]_2$ as does happen when reaction of **1** with $[IrCp^*Cl_2]_2$ takes place in thf-d_6 with 3.5 molar equivalents of acetone. However, since only **2** is observed when acetone is the solvent, we have re-considered the pathway for formation of imine, or intermediate **A** in Pathway II, and search for a possible rationalization.

Mechanism for the imine formation catalyzed by $CpIrCl_2$. The formation of the imine comes from the condensation of the amine with acetone with loss of water. The electrophilicity of acetone is increased following coordination of the oxygen to a Lewis acid, which in this reaction can be the Ir catalyst. As has been described in the experimental section above, acetone is required to dissociate the dinuclear $[Cp^*IrCl_2]_2$ and to form the mononuclear acetone adduct $[Cp^*IrCl_2(acetone)]$, modelled by **o1** (Scheme 5). Species **o1** is 8.9 kcal mol^{-1} less stable than **a1** and 1.6 kcal mol^{-1} more stable than **a2**. This energy pattern is obtained considering stoichiometric conditions with equal quantities of the amine **1** and acetone. This is not a realistic model of the experimental conditions; the large excess of acetone, used as solvent, should displace the equilibrium in favor of **o1**, and thus, the concentration of **o1** could dominate over **a2** and compete with **a1**. So, **o1** should be considered as a possible intermediate in the formation of the imine. Calculations show that this result does not change on considering other possible complexes in which one of the chlorides has been replaced by a neutral ligand such as acetone (details in the ESI†).

We then considered an iridium assisted formation of the imine using **o1** and the amine as the starting reactants, as depicted in Scheme 6. The first step is the nucleophilic addition of the amine **1** to the activated acetone. This step, with an energy barrier of 10 kcal mol^{-1} (**TSo1-2**), gives intermediate **o2** with an acidic proton bound to N. From this species two proton migrations from nitrogen to oxygen giving finally H_2O and coordinated imine (**i1** or **A** in Fig. 1) can occur. These proton transfers can take place through intermediates **o2** and **o3** with energies under 20 kcal mol^{-1}. The proton transfer between **o2**, **o3**, **o4** and the loss of water have not been studied in further detail. Such steps are well known, and probably take place with the assistance of acetone with low energy barriers as shown in the case of the amine proton transfer (**TSa3-4ass**).

Using these results, we propose that when the reaction takes place in pure acetone the iridium fragment coordinates preferentially to acetone rather than the amine by η^2 coordination. As a consequence, the amine reacts preferentially with the coordinated acetone to form the imine and not with the iridium fragment to form the non-vinylic indole, **3**. In other words the large excess of acetone blocks the regular hydroamination process and only allows the formation of **2**.

Proposed mechanism for the formation of 2. From the computational studies and the comparison with experimental data, a detailed catalytic cycle, slightly different from Pathway II proposed in Fig. 1, is shown in Scheme 7. The first step is the fragmentation of $[Cp^*IrCl_2]_2$ by acetone. Two Lewis bases can compete with

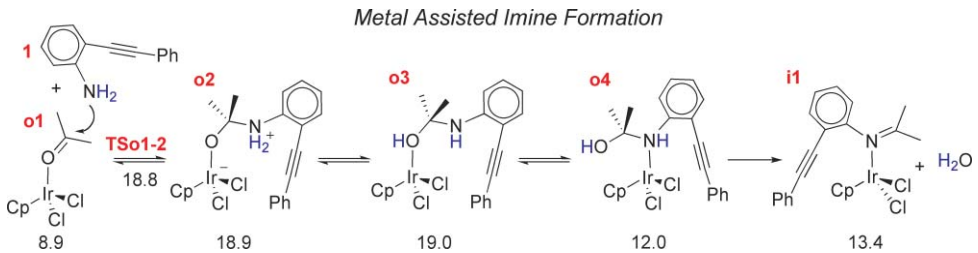

Scheme 6 Mechanism proposed for the imine formation assisted by $[CpIrCl_2]$ complex. Energies are given relative to **a1**, in kcal mol^{-1} and include the solvent (acetone) effect.

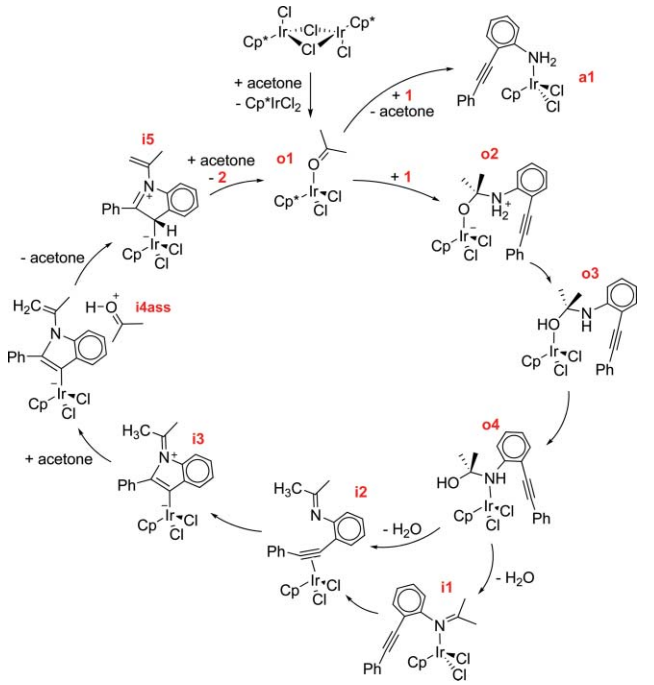

Scheme 7 Catalytic cycle proposed for the reaction of **1** with acetone to give **2**, catalyzed by $[Cp^*IrCl_2]_2$.

the empty coordination site of $CpIrCl_2$; the phenyl amine is the strongest base and it gives complex **a1** (model of **4**), with amine κ^1(N) coordinated, but acetone, which is in large excess, may favor formation of the acetone complex **o1**. The latter complex has an electrophilically active carbon, which can react with the amine. After several proton shuffles and loss of water, an imine **i1** is formed. This imine can easily exchange from κ^1-N to η^2-CC coordination (**i1** to **i2**). The η^2-CC coordinated imine has an activated alkyne and reactive N center which results in the cyclisation with an accessible energy barrier and the formation of a vinyl indole ring metallated at the C3 position. The resulting compound **i3** is neutral but is both a strong acid at the methyl of the iminium group and a strong base through the metallated C3 carbon. Intramolecular proton transfers are found to have prohibitively high energy barriers. Loss of proton to the solvent (acetone) and subsequent protonation would be preferred. This will lead to the product **i5** with a favorable energy of reaction and account for the selective deuteration at C3 of the indole **2**. The liberated $CpIrCl_2$ species is coordinated by acetone, once again forming the catalyst and continuing with the catalytic cycle.

This new catalytic cycle shows the importance of acetone in the formation of **2**. Thus, acetone participates in the fragmentation of complex $[Cp^*IrCl_2]_2$. By coordination of Ir, it blocks the formation of the η^2(CC) bonded aniline, **a2**. Acetone is one of the reactants in the imine formation and it also participates in the proton transfer that takes place in the imine cyclisation. This accounts for the experimental results observed when different amounts of acetone are used. When 1 reacts with $[Cp^*IrCl_2]_2$ in thf-d_8 there is no reaction because acetone is required for the Ir complex fragmentation. However, **1** does not react with $[Cp^*IrCl_2$(aniline-κN)] (**4**) in CD_2Cl_2 probably because acetone is also needed for the proton transfer. The reaction of **1** with $[Cp^*IrCl_2]_2$ and 3.5 molar equivalents of acetone gives **2** and **3** in a 1:2 molar ratio. It seems that this amount of acetone is enough to give fragmentation, formation of imine and proton transfer leading **2** and **3**, but it is not enough to completely avoid the formation of **a2**, which subsequently leads to the formation of **3**.

Conclusions

This combined experimental computational study of the unusual formation of vinyl indole by the reaction of 2-(2-phenylethynyl)aniline with acetone in presence of $[IrCp^*Cl_2)_2$ suggests a mechanistic route, in which acetone plays a key role in several steps of the multistep pathways. It participates in the fragmentation of the dinuclear Ir complex and the formation of the reactive form of the catalyst. It blocks the formation of the expected hydroamination product by coordination to the Ir catalyst. Coordinated acetone reacts with the aniline to form an imine derivative, which yields the final product after proton transfer helps by acetone itself. This mechanistic proposal accounts for all experimental data carried out to analyze this mechanistic issue.

Experimental

General procedures

Reagents were purchased from Aldrich and used as received unless otherwise stated. All solvents were pre-dried and distilled under an atmosphere of argon. Acetone and acetone-d_6 were dried with $CaSO_4$ and distilled under argon prior to use. Methanol was dried over 4 Å molecular sieves and distilled from CaH_2. Thf-d_8 was dried over sodium/benzophenone and distilled prior to use. 1,1,2,2-Tetrachloroethane was dried with $CaSO_4$ and distilled under argon. 1,2,3,4,5-Pentamethylcyclopentadiene was purchased from Lancaster and used without further purification. Iridium(III) chloride hydrate was obtained from Precious Metals Online (PMO) and used without further purification. $[IrCp^*Cl_2]_2$ was synthesised according to the literature.[23] ^{1}H NMR spectra were recorded on a Bruker DMX500 spectrometer. All spectra were recorded at 323 K unless otherwise specified. ^{1}H NMR chemical shifts were referenced internally to residual solvent resonances. MS was performed by Biomedical Mass Spectrometry Facility at the University of New South Wales, Sydney and X-Ray Crystallographic analysis was performed by Dr Anthony Willis at the Research School of Chemistry, Australian National University, Canberra.

X-ray crystallography

Diffraction images were measured at 200 K on a Nonius KappaCCD diffractometer (MoKα, graphite monochromator, λ = 0.71073 Å) and data extracted using the DENZO package.[24] The structure was solved by direct methods (SIR92),[25] and refined using the CRYSTALS program package.[26] The displacement ellipsoid diagram was prepared with use of ORTEP-II.[27]

Crystal data: orange block, 0.26 × 0.11 × 0.09 mm, $C_{24}H_{26}Cl_2IrN.CH_2Cl_2$, M_r = 676.53, orthorhombic, space group $P2_12_12_1$, a = 8.8981 (1), b = 11.8148 (2), c = 24.1539 (3) Å, V = 2539.28 (6) Å^3, Z = 4, D_x = 1.770 g cm^{-3}, μ = 56.92 cm^{-1}. 29393 reflections measured, $2\theta_{max}$ = 55°, h = −11 → 11, k = −15 → 15,

$l = -31 \rightarrow 31$, analytical absorption correction applied: $T_{min} = 0.367$, $T_{max} = 0.661$, 5831 independent reflections, $R_{int} = 0.028$.

Full matrix least squares refinement on F^2, Chebychev polynomial weighting scheme,[28,29] R(5566 reflections with $I > 2\sigma(I)$) = 0.0163, wR(all data) = 0.0302, S = 0.9414, Flack parameter = –0.019 (4), $\Delta\rho_{max} = 0.79$, $\Delta\rho_{min} = -1.00$ e Å^{-3}.

General procedure for the catalysed cyclisation of 1

The cyclisation of **1** to give **2**, as catalysed by $[IrCp^*Cl_2]_2$, was performed on a small scale in an NMR tube fitted with Young's concentric Teflon valves. The substrate and catalyst were weighed and the solvent was vacuum transferred into the tube. The tube was placed under argon and a known amount of 1,1,2,2-tetrachloroethane (*ca.* 50 mg) was added as an internal standard. All reactions were performed with approximately 5 mol% catalyst loading (w.r.t. Ir) at 50 °C by heating the tube within the probe of the NMR spectrometer. The temperature within the magnet was calibrated using ethylene glycol. ^{1}H NMR spectra were recorded and the conversion to *N*-(2-methylvinyl)-2-phenylindole **2** was determined by integration of the product resonance (at 7.82 ppm) relative to the internal standard (at 6.55 ppm). Conversion of > 95% is taken as the time where no remaining substrate resonances were evident.

Reaction of 2-phenylindole 3 and acetone in the presence of $[IrCp^*Cl_2]_2/NaBF_4$

2-Phenylindole **3** (103.5 mg, 0.522 mmol), $[IrCp^*Cl_2]_2$ (10.1 mg, 0.0126 mmol) and $NaBF_4$ (8.4 mg, 0.0766 mmol) were dissolved in acetone (5 mL) and heated at 50 °C for 18 hours under an atmosphere of argon. The solvent was removed *in vacuo* and analysis of the crude reaction mixture by ^{1}H NMR spectroscopy in acetone-d_6 showed no conversion or decomposition of the 2-phenylindole **3**.

Isolation of $[IrCl_2$(aniline-κ*N*)$Cp^*]$ 4

Under argon **1** (828 mg, 4.28 mmol), $[IrCp^*Cl_2]_2$ (209 mg, 0.262 mmol) and $NaBF_4$ (34 mg, 0.31 mmol) were dissolved in 10 mL acetone. The mixture was heated at reflux at 55 °C for 18 h. The solution was cooled and the reaction mixture filtered. The yellow solid obtained was isolated and recrystallised by slow diffusion of pentane into a concentrated CH_2Cl_2 solution. After one week orange crystals were obtained (45.3 mg, 0.0771 mmol, 29%). The compound was identified to be the substrate bound to the Ir metal centre generating the complex [Cp*IrCl$_2$(2-(2-phenylethynyl)aniline)]. The orange crystals obtained were suitable for X-ray crystallographic analysis. $C_{24}H_{26}Cl_2IrN{\cdot}CH_2Cl_2$ (676.54): calcd. C, 44.38; H, 4.17; N, 2.07; found: C, 45.25; H, 4.32; N, 2.35 %. MS (ES$^+$) *m/z:* 593 (M$^+$, 10%), 556 (M–Cl, 80%), 520 (M–2Cl, 100%). ^{1}H NMR (CD_2Cl_2, 300 MHz, 298 K): δ 7.72 (m,1H, H6), 7.52 (m, 1H, H3), 7.46-7.31 (m, 6H, H5 + Ph), 7.15 (m, 1H, H4), 5.84 (br s, 2H, NH_2), 1.38 (s, 15H, Cp*) ppm. ^{13}C NMR (CD_2Cl_2, 75 MHz, 298 K): δ 145.0 (C2), 132.4 (C6), 132.0 (C4), 130.2 (C5), 129.6 (Ph), 129.1 (Ph), 125.3 (C4), 122.8 (i-Ph), 120.6 (Ph), 115.4 (C1), 98.0 (C≡C), 86.1 (Cp) 86.2 (C≡C), 9.1 (Cp–Me) ppm.

The filtrate was purified on a small silica column using Et_2O: Light Petroleum (1:1) as eluent to remove remaining Ir compounds. The compound **4** was isolated as a beige solid (143 mg, 0.7 mmol, 16% Yield). Despite complete conversion to the vinyl indole **2** significant amounts of 2-phenylindole **3** were also isolated due to decomposition during chromatography. The compound **2** was found to be unstable in acidic solutions losing the vinyl group generating 2-phenylindole **3** which was identified by comparison of the ^{1}H NMR data obtained to that of a true sample of 2-phenylindole. The characterisation of this compound has been reported previously.[19]

Computational details

DFT calculations were carried out using the hybrid B3PW91 functional.[30] Two different basis set, I and II, were used. Basis set I (ECP-adapted SDDALL[31] with a set of polarization functions for Ir[32] and Cl[33] and the all-electron 6-31G(d,p)[34] for N, O, C, and H) was used to optimize the geometries, and basis set II (the same as I but using the all-electron 311+G(d,p)[35] for N, O, C, and H) to refine the energies of stationary points through single-point calculations. Geometry optimizations were carried out without any geometrical constraints. The nature of all stationary points was confirmed by an analytical calculation of frequencies. Each transition state was relaxed toward reactant and product using the analytical vibrational data to confirm its nature. The effect of the acetone solvent (ε = 20.7), was evaluated using the continuum IEFPCM model.[36] All energies given in the text include the solvent effect and were obtained with basis set II. All calculations were carried out with the Gaussian03 package.[37] The geometries of intermediates and transition states having no remarkable features are not presented in the paper. These structures are available in the ESI.†

We considered that the dinuclear Ir complex splits into two monomers which was modelled by $CpIrCl_2$, where Cp = C_5H_5 and we did not analyze the formation of $CpIrCl_2$. All organic reactants were modelled in full.

Acknowledgements

We gratefully acknowledge financial support from The University of New South Wales and The Australian Research Council. We also thank the Australian government for an Australian Postgraduate Award (D.F.K.). BAM and OE thank the RSC for international grants for authors. A.N. thanks the Spanish MICINN for a MEC postdoctoral fellowship. The authors thank S.A. Macgregor (Heriot Watt University, UK) and D. St Claire Black (UNSW, Australia) for useful discussions.

References

1 *Indoles*, ed. R. J. Sundberg, Academic Press, London, 1996.
2 G. W. Gribble, *Comprehensive Heterocyclic Chemistry II*, ed. A. R. Katritzky, C. W. Ress, E. F. V. Scriven and C. W. Bird, Pergamon Press, Oxford, 1996, Vol. 2, p. 207.
3 D. A. Horton, G. T. Bourne and M. L. Smythe, *Chem. Rev.*, 2003, **103**, 893–930 and references therein.
4 G. R. Humphrey and J. T. Kuethe, *Chem. Rev.*, 2006, **106**, 2875–2911.
5 R.J. Sundberg, Pyrroles and Their Benzoderivatives: Synthesis and Applications. In *Comprehensive Heterocyclic Chemistry*, A. R. Katritzky and C. W. Rees, Eds., Pergamon, Oxford, U.K., 1984, Vol. 4, pp 313-376.
6 P. Burger and R. G. Bergman, *J. Am. Chem. Soc.*, 1993, **115**, 10462–10463.

7 D. M. Tellers and R. G. Bergman, *Organometallics*, 2001, **20**, 4819–4832.
8 X. Li, T. Vogel, C. D. Incarvito and R. H. Crabtree, *Organometallics*, 2005, **24**, 62–76.
9 X. Li, A.R. Chianese, T. Vogel and R. H. Crabtree, *Org. Lett.*, 2005, **7**, 5437–5440.
10 N. A. Wynberg, L. J. Leger, M. L. Conrad, C. M. Vogels, A. Decken, S. J. Duffy and S. A. Wescott, *Can. J. Chem.*, 2005, **83**, 661–667.
11 K-I. Fujita, Z. Li, N. Ozeki and R. Yamaguchi, *Tetrahedron Lett.*, 2003, **44**, 2687–2690.
12 D. Balcells, A. Nova, E. Clot, D. Gnanamgari, R. H. Crabtree and O. Eisenstein, *Organometallics*, 2008, **27**, 2529–2535.
13 M. Furegati and A. J. Rippert, *Tetrahedron: Asymmetry*, 2005, **16**, 3947–3950.
14 K-I. Fujita, C. Kitatsuji, S. Furukawa and R. Yamaguchi, *Tetrahedron Lett.*, 2004, **45**, 3215–3217.
15 F. Brustolin, V. Castelvetro, F. Ciardelli, G. Ruggeri and A. Colligiani, *J. Polym. Sci., Part A: Polym. Chem.*, 2001, **39**, 253–262.
16 Y. Zhang, J. P. Donahue and C.-J. Li, *Org. Lett.*, 2007, **9**, 627–630.
17 M. Movassaghi and A. E. Ondrus, *J. Org. Chem.*, 2005, **70**, 8638–8641.
18 A. Y. Lebedev, V.V. Izmer, D. N. Kazyul'kin, I. P. Beletskaya and A. Z. Voskoboynikov, *Org. Lett.*, 2002, **4**, 623–626.
19 D. F. Kennedy, B. A. Messerle and S. L. Rumble, *New J. Chem.*, 2009, **33**, 818–824.
20 D. L. Davies, O. Al-Duaij, J. Fawcett, M. Giardiello, S. T. Hilton and D. R. Russell, *Dalton Trans.*, 2003, 4132–4138.
21 Similar results were obtained with other systems such as cationic species were one chloride is replaced by acetone $[CpIrCl(acetone)]^+$ (see ESI†).
22 G. Kovacs, G. Ujaque and A. Lledos, *J. Am. Chem. Soc.*, 2008, **130**, 853–864.
23 C. White, A. Yates and P. M. Maitlis, *Inorg. Synth.*, 1992, **29**, 228.
24 Z. Otwinowski and W. Minor (1996). *Processing of X-ray Diffraction Data Collected in Oscillation Mode. Methods Enzymol.* Eds C. W. Carter and R. M. Sweet, Academic Press. 1997, 276, 307-326.
25 A. Altomare, G. Cascarano, C. Giacovazzo, A. Guagliardi, M. C. Burla, G. Polidori, G. and M. Camalli, *J. Appl. Crystallogr.*, 1994, **27**, 435–435.
26 P. W. Betteridge, J. R. Carruthers, R. I. Cooper, K. Prout and D. J. Watkin, *J. Appl. Crystallogr.*, 2003, **36**, 1487–1487.
27 C. K. Johnson, *ORTEP–II, A Fortran Thermal-Ellipsoid Plot Program*, Report ORNL-5138, Oak Ridge National Laboratory, Oak Ridge, Tennessee, USA, 1976.
28 D. J. Watkin, *Acta Crystallogr., Sect. A: Found. Crystallogr.*, 1994, **50**, 411–437.
29 E. Prince, *Mathematical Techniques in Crystallography and Materials Science*, Springer-Verlag, New York, 1982.
30 (*a*) A. D. Becke, *J. Chem. Phys.*, 1993, **98**, 5648; (*b*) J. P. Perdew and Y. Wang, *Phys. Rev. B: Condens. Matter Mater. Phys.*, 1992, **45**, 13244.
31 (*a*) D. Andrae, U. Haüssermann, M. Dolg, H. Stoll and H. Preuss, *Theor. Chim. Acta*, 1990, **77**, 123; (*b*) A. Bergner, M. Dolg, W. Küchle, H. Stoll and H. Preuss, *Mol. Phys.*, 1993, **80**, 1431.
32 A. W. Ehlers, M. Böhme, S. Dapprich, A. Gobbi, A. Höllwarth, V. Jonas, K. F. Köhler, R. Stegmann, A. Veldkamp and G. Frenking, *Chem. Phys. Lett.*, 1993, **208**, 111.
33 A. Höllwarth, H. Böhme, S. Dapprich, A. W. Ehlers, A. Gobbi, V. Jonas, K. F. Köhler, R. Stegmann, A. Veldkamp and G. Frenking, *Chem. Phys. Lett.*, 1993, **208**, 237.
34 P. C. Hariharan and J. A. Pople, *Theor. Chim. Acta*, 1973, **28**, 213.
35 M. J. Frisch, J. A. Pople and J. S. Binkley, *J. Chem. Phys.*, 1984, **80**, 3265.
36 (*a*) M. T. Cancès, B. Mennucci and J. Tomasi, *J. Chem. Phys.*, 1997, **107**, 3032; (*b*) M. Cossi, V. Barone, B. Mennucci and J. Tomasi, *Chem. Phys. Lett.*, 1998, **286**, 253; (*c*) B. Mennucci and J. Tomasi, *J. Chem. Phys.*, 1997, **106**, 5151.
37 M. J. Frisch, G. W. Trucks, H. B. Schlegel, G. E. Scuseria, M. A. Robb, J. R. Cheeseman, J. A. Montgomery, Jr., T. Vreven, K. N. Kudin, J. C. Burant, J. M. Millam, S. S. Iyengar, J. Tomasi, V. Barone, B. Mennucci, M. Cossi, G. Scalmani, N. Rega, G. A. Petersson, H. Nakatsuji, M. Hada, M. Ehara, K. Toyota, R. Fukuda, J. Hasegawa, M. Ishida, T. Nakajima, Y. Honda, O. Kitao, H. Nakai, M. Klene, X. Li, J. E. Knox, H. P. Hratchian, J. B. Cross, V. Bakken, C. Adamo, J. Jaramillo, R. Gomperts, R. E. Stratmann, O. Yazyev, A. J. Austin, R. Cammi, C. Pomelli, J. Ochterski, P. Y. Ayala, K. Morokuma, G. A. Voth, P. Salvador, J. J. Dannenberg, V. G. Zakrzewski, S. Dapprich, A. D. Daniels, M. C. Strain, O. Farkas, D. K. Malick, A. D. Rabuck, K. Raghavachari, J. B. Foresman, J. V. Ortiz, Q. Cui, A. G. Baboul, S. Clifford, J. Cioslowski, B. B. Stefanov, G. Liu, A. Liashenko, P. Piskorz, I. Komaromi, R. L. Martin, D. J. Fox, T. Keith, M. A. Al-Laham, C. Y. Peng, A. Nanayakkara, M. Challacombe, P. M. W. Gill, B. G. Johnson, W. Chen, M. W. Wong, C. Gonzalez and J. A. Pople, *GAUSSIAN 03 (Revision E.1)*, Gaussian, Inc., Wallingford, CT, 2004.

